

Fast Capacity Estimation in Ultra-dense Wireless Networks with Random Interference

Dandan Jiang, Rui Wang, and Jiang Xue[✉], *Member, IEEE*

Abstract

In wireless communication systems, the accurate and reliable evaluation of channel capacity is believed to be a fundamental and critical issue for terminals. However, with the rapid development of wireless technology, large-scale communication networks with significant random interference have emerged, resulting in extremely high computational costs for capacity calculation. In ultra-dense wireless networks with extremely large numbers of base stations (BSs) and users, we provide fast estimation methods for determining the capacity. We consider two scenarios according to the ratio of the number of users to the number of BSs, β_m . First, when $\beta_m \leq 1$, the Fisher-Spiked Estimation (FISE) algorithm is proposed to determine the capacity by modeling the channel matrix with random interference as a Fisher matrix. Second, when $\beta_m > 1$, based on a closed-form expression for capacity estimation requiring solely simple computations, we prove that this estimation stabilizes and remains invariant with increasing β_m . Our methods can guarantee high accuracy on capacity estimation with low complexity, which is faster than the existing methods. Furthermore, our approaches exhibit excellent generality, free of network area shapes, BS and user distributions, and sub-network locations. Extensive simulation experiments across various scenarios demonstrate the high accuracy and robustness of our methods.

Index Terms

future wireless systems, capacity estimation, random matrix theory, spiked Fisher matrix

I. INTRODUCTION

The channel capacity, defined as the maximum achievable rate at which information can be transmitted through a channel, plays a significant role in wireless communication systems. Accurate and reliable evaluation of channel capacity is considered as a fundamental and critical

Dandan Jiang, Rui Wang and Jiang Xue are with School of Mathematics and Statistics, Xi'an Jiaotong University, Xi'an, China (e-mail: jiangdd@xjtu.edu.cn; wangrui_math@stu.xjtu.edu.cn; x.jiang@xjtu.edu.cn). (Corresponding author: Jiang Xue.)

issue for terminal performance. As mobile communication technology improves by leaps and bounds, increasingly intricate wireless systems emerge, posing the challenge of determining the capacity with low complexity and high accuracy. As a pioneering work, Dr. Claude E. Shannon originally proposed the definition of channel capacity and provided its calculation method [1], which is known as the Shannon-Hartley theorem. Based on this theorem, the capacity of an additive white Gaussian noise (AWGN) channel with bandwidth W can be calculated by $C = W \log(1 + P/(N_0W))$ [2], where P denotes signal power and N_0 represents noise power. Subsequently, the growing demand for increased transmission capacity has propelled the development of multiple-input multiple-output (MIMO) antennas. As detailed in [3], the capacity of a multi-user (MU)-MIMO channel with t transmission antennas and r receiving antennas can be expressed as follows:

$$C = \mathbb{E} \left\{ \log \det \left(\mathbf{I} + \frac{P}{t} \mathbf{H} \mathbf{H}^* \right) \right\}, \quad (1)$$

where \mathbf{H} is the channel gain matrix, and $(\cdot)^*$ represents the Hermitian transpose. The notations \mathbb{E} and $\det(\cdot)$ represent the expectation and the determinant of a matrix, respectively. When t and r are large, the expression in (1) requires the determinant calculation of a large-dimensional matrix, consuming substantial computational resources. Existing methods for direct computation of C in (1), such as Cholesky decomposition and singular value decomposition (SVD), have a complexity of $O(t^3)$, which is unacceptable for future ultra-dense networks.

Recently, to further enhance the capacity of wireless channels, a capacity-centric (C^2) network architecture has been designed for future wireless communications [4]. The C^2 architecture divides the whole network into M non-overlapping clusters, each operating in parallel. Only the base stations (BSs) within each cluster collaborate to serve nearby users, and there is non-negligible interference among different clusters. Its average uplink capacity of the m -th cluster per BS can be obtained by [4]

$$C_m = \mathbb{E} \left\{ \frac{1}{J_m} \log \det \left(\mathbf{I} + P \mathbf{\Xi}_m^{-1} \mathbf{H}_m \mathbf{H}_m^* \right) \right\}, \quad (2)$$

where J_m^1 is the number of BSs in the m -th cluster, \mathbf{H}_m and $\mathbf{\Xi}_m$ denote the channel gain matrix and the noise-plus-interference matrix in this cluster, respectively. Additionally, $P \mathbf{\Xi}_m^{-1} \mathbf{H}_m \mathbf{H}_m^*$ represents the signal to the interference plus noise ratio (SINR) matrix of the m -th cluster. It

¹In this paper, we only consider the situation of single-antenna BS. For multi-antenna BS, J_m can also represent the total number of antennas within the m -th cluster.

can be seen that (2) is more general and more complicated than (1), since the C^2 network can be seen as a multiple MU-MIMO channel with inter-cluster interference. Moreover, we note that there are several other architectures in the literature that are built similarly to C^2 , such as clustered cell-free [5], CGN [6], and others [7]–[9]. Their capacity expressions are consistent with formula (2), making the methods presented in this paper applicable to these architectures as well.

Many approaches have been developed to tackle capacity calculations involving large-dimensional channel matrices, diverging from conventional determinant-calculation-based methods. [10] utilized the random matrix theory (RMT) to derive the asymptotic channel capacity with implicit expressions as the number of BSs and users increases, which are mostly applicable to channels using code-division multiple access schemes, restricting their extension to other models. Moreover, several works are specifically dedicated to determining the capacity in (2), such as [4], [11], [12]. In [4], a closed-form estimation for C_m was provided based on the convergence of the SINR matrix to a diagonal matrix under some asymptotic conditions. The TOSE method in [11] used the limiting spectral theory of spiked covariance matrix to achieve fast eigenvalues estimation, but it relies on an assumption that the noise-plus-interference matrix Ξ_m is deterministic, inconsistent with the inherent randomness of Ξ_m in practical scenarios. In addition, the accuracy of this method is also unstable for a channel matrix with extremely uneven signal descend. The MPM method introduced in [12] was developed to estimate the capacity by approximating the spectral distribution of the SIRM matrix in (2). Notably, all of the above methods ([4], [11], [12]) rely on the assumption that the matrix Ξ_m converges to a diagonal form as the number of users approaches infinity. However, as discussed in [13], the convergence of large-dimensional matrices is not equivalent to the convergence of their spectra. Therefore, these capacity estimations increasingly deviate from reality as β_m decreases, where β_m represents the ratio of the number of users to the number of BSs in the m -th cluster. Consequently, a method for determining the capacity that can simultaneously guarantee high accuracy, low complexity, and superior generality needs to be further explored.

In this paper, we propose fast estimation methods for calculating capacity in ultra-dense wireless networks with random interference, effectively avoiding the high complexity in conventional determinant-calculation-based methods. We consider two cases: $\beta_m \leq 1$ and $\beta_m > 1$. When $\beta_m \leq 1$, the Fisher-Spiked Estimation (FISE) algorithm is proposed to fast and accurately estimate C_m in (2), which employs the limiting spectral theory of spiked Fisher matrix to realize

a fast estimation of eigenvalues. When $\beta_m > 1$, based on the capacity estimation \tilde{C}_m proposed by [4] and detailed later in formula (18), we further prove that this estimation reaches a constant value that is independent of β_m . The major contributions of this work can be concluded in terms of the following.

- (a) The FISE algorithm is of low complexity with high accuracy in capacity estimation. Different from the existing methods, FISE eliminates the diagonal assumption of Ξ_m and instead adopts its true structure. The proposed estimation also preserves the randomness of the interference matrix, which aligns more closely with real-world case. In terms of computational complexity, when provided with the SINR matrix, the complexity for FISE itself amounts to only $O(J_m)$, which is less than the existing methods.
- (b) The stability of the average cluster capacity estimation for $\beta_m > 1$ is proved. Specifically, based on the closed-form estimation \tilde{C}_m provided by [4], we demonstrate that this estimation is a constant that does not rely on the value of β_m . Thus, when $\beta_m > 1$, we do not need to repeat the capacity calculation and can instead use this stable constant, significantly saving computing power resources.
- (c) Our proposed methods exhibit remarkable generality, which are free of nodes (BSs and users) distributions, network area shapes, and the locations of clusters within the network. In the simulation experiments, both square and round network regions were designed, along with two types of nodes distributions. Besides, three clusters with representative locations were chosen to calculate the channel capacity. The experimental results indicate that the our methods perform well across various scenarios.

The arrangement of the following content is as below. First, the system model is formulated in Section II. Section III elaborates on the procedures of FISE to determine the capacity based on the spiked Fisher matrix when $\beta_m \leq 1$. Section IV introduces a computationally simple expression for capacity estimation when $\beta_m > 1$ and proves its stability. As a by-product, an explicit expression of the average cluster capacity estimation per BS with a constant user density is also derived. Section V shows simulation results on the capacity estimation comparison between our proposed methods and other existing methods under different scenarios. Finally, Section VI draws the conclusion.

Notations: We use the following notations throughout this paper: Lower case, boldface lower case, and boldface upper case letters represent scalars, vectors, and matrices, respectively, like

h , \mathbf{h} , and \mathbf{H} . The (i, j) -th entry of \mathbf{H} is denoted by $[\mathbf{H}]_{ij}$. Scripts such as \mathcal{B} represent the sets. Operator $\mathcal{CN}(\mu, \nu)$ is a complex Gaussian distribution with mean μ and covariance ν . $\|\cdot\|_F$ and $|\cdot|$ represent the Frobenius norm and the absolute value. Moreover, other operators $\text{tr}(\cdot)$, $(\cdot)^*$, $\det(\cdot)$, $\mathbb{E}\{\cdot\}$, and $(\cdot)^{-1}$ represent the trace, Hermitian transpose, determinant, expectation, and matrix inverse, respectively.

II. MODELING THE SYSTEM WITH RANDOM INTERFERENCE

In this section, we introduce the system model for C² networks proposed in [4] considering massive random interference. The network is comprised of two types of nodes: (1) J single-antenna BSs (or access points in distributed-antenna systems [14], [15]), which is denoted by $\mathcal{B} = \{b_1, b_2, \dots, b_J\}$; (2) K single-antenna users, which is denoted by $\mathcal{U} = \{u_1, u_2, \dots, u_K\}$. Suppose the entire network is decomposed into M non-overlapping clusters, each operating in parallel. The schematic diagram is depicted in Fig. 1, where each color represents a separate cluster, circles represent BSs, and triangles represent users. The cluster marked by the black pentagon is denoted as the m -th cluster, used as a target to calculate the capacity. For the m -th cluster, let \mathcal{C}_m represent the union of the sets of BSs and users in this cluster, thus $\bigcup_{m=1}^M \mathcal{C}_m = \mathcal{B} \cup \mathcal{U}$. Furthermore, denote the number of BSs in \mathcal{C}_m as J_m and the number of users as K_m . To reflect the ultra-dense scenario of the network, we assume that $J_m, K_m \rightarrow \infty$.

The channel gain between the BS $b_j \in \mathcal{C}_m$ and the user $u_k \in \mathcal{U}$ is modeled by

$$h_{mjk} = l_{mjk} g_{mjk},$$

where $g_{mjk} \sim \mathcal{CN}(0, 1)$ is the small-scale fading, and

$$l_{mjk} = \begin{cases} d_{mjk}^{-1.75}, & d_{mjk} > d_1 \\ d_1^{-0.75} d_{mjk}^{-1}, & d_0 < d_{mjk} \leq d_1 \\ d_1^{-0.75} d_0^{-1}, & d_{mjk} \leq d_0 \end{cases} \quad (3)$$

is the large-scale fading [16]. Here, d_{mjk} is the Euclidean distance between the BS $b_j \in \mathcal{C}_m$ and the user u_k . d_0 and d_1 are the near-field threshold and far-field threshold, respectively.

The uplink signal model of the m -th cluster is given by

$$\mathbf{y}_m = \sum_{u_k \in \mathcal{C}_m} \mathbf{h}_{mk} s_k + \sum_{u_k \notin \mathcal{C}_m} \mathbf{h}_{mk} s_k + \mathbf{u}_m, \quad (4)$$

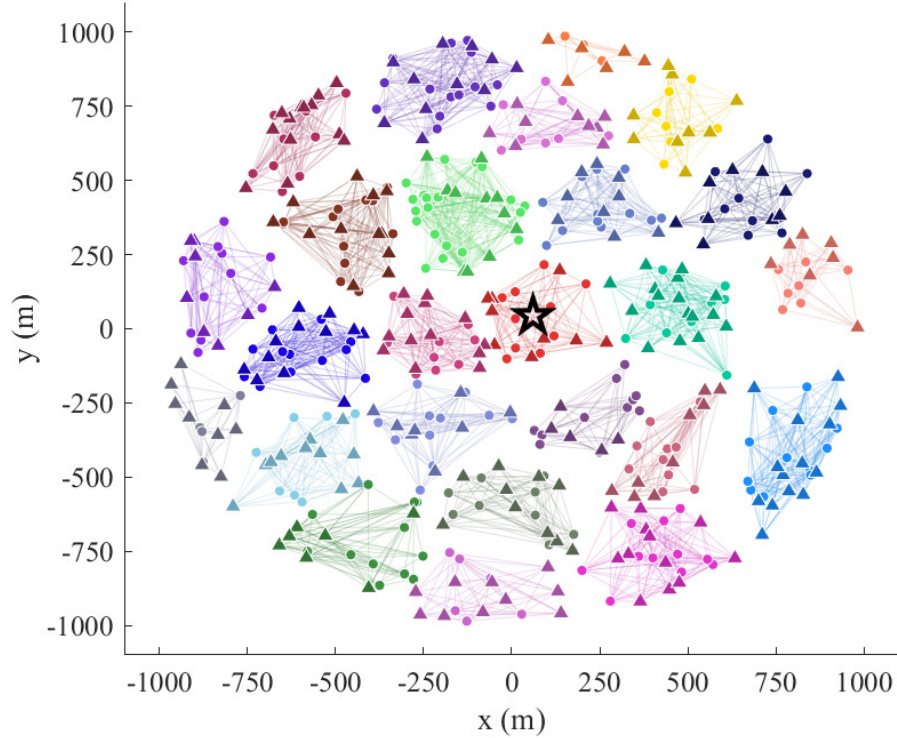


Fig. 1. Schematic diagram of the wireless network. Different colors represent different clusters. Circles are BSs, triangles are users. The cluster marked by the black pentagon is the closest to the center of the network.

where \mathbf{h}_{mk} is a $J_m \times 1$ vector with h_{mjk} as its j -th element, $s_k \sim \mathcal{CN}(0, P)$ is the signal of the user u_k , with P being the transmit power of each user. Moreover, $\mathbf{u}_m \sim \mathcal{CN}(0, N_0\mathbf{I})$ is the AWGN vector. Define the channel gain matrix \mathbf{H}_m as

$$\mathbf{H}_m = \mathbf{L}_m \circ \mathbf{G}_m,$$

where $\mathbf{L}_m \in \mathbb{R}^{J_m \times K_m}$ is the large-scale fading matrix, $\mathbf{G}_m \in \mathbb{C}^{J_m \times K_m}$ is the small-scaling fading matrix, with their (j, k) -th entries given by $[\mathbf{L}_m]_{jk} = l_{mjk}$ and $[\mathbf{G}_m]_{jk} = g_{mjk}$. Here, \circ represents the Hadamard product. Besides, represent the noise-plus-interference matrix as

$$\mathbf{\Xi}_m = N_0\mathbf{I} + P \sum_{u_k \notin \mathcal{C}_m} \mathbf{h}_{mk}\mathbf{h}_{mk}^*. \quad (5)$$

Thus, the average capacity of cluster m per BS can be obtained as referred in [1], [17]

$$\begin{aligned} C_m &= \mathbb{E} \left\{ \frac{1}{J_m} \log \det \left(\mathbf{I} + P\mathbf{\Xi}_m^{-1/2}\mathbf{H}_m\mathbf{H}_m^*\mathbf{\Xi}_m^{-1/2} \right) \right\} \\ &= \mathbb{E} \left\{ \frac{1}{J_m} \log \det \left(\mathbf{I} + P\mathbf{\Xi}_m^{-1/2}(\mathbf{L}_m \circ \mathbf{G}_m)(\mathbf{L}_m \circ \mathbf{G}_m)^*\mathbf{\Xi}_m^{-1/2} \right) \right\}. \end{aligned} \quad (6)$$

In existing works, people usually consider only the randomness of the target channel matrix while regarding the interference matrix as fixed, which leads to the network system not adapting to real-time dynamic changes, and also brings unstable capacity estimation errors. To address this issue, our modeling process treats both the target channel matrix and interference matrix as random matrices. Define $\mathbf{B}_m = P\mathbf{\Xi}_m^{-1/2}(\mathbf{L}_m \circ \mathbf{G}_m)(\mathbf{L}_m \circ \mathbf{G}_m)^*\mathbf{\Xi}_m^{-1/2}$. We can rewrite $\mathbf{I} + \mathbf{B}_m$ in the form of $\mathbf{\Sigma}_1\mathbf{\Sigma}_2^{-1}$, where $\mathbf{\Sigma}_1 = \mathbf{\Sigma}_2 + \mathbf{\Delta}$ and $\mathbf{\Delta} = \mathbf{B}_m\mathbf{\Sigma}_2$. As a result, the matrix $\mathbf{I} + \mathbf{B}_m$ in (6) is characterized as the ratio of two random covariance matrices, fitting the typical structure of Fisher matrices in RMT. Furthermore, $\mathbf{I} + \mathbf{B}_m$ always presents the dominant advantage of the first few eigenvalues, which is the so-called spiked property. To be specific, the matrix $\mathbf{I} + \mathbf{B}_m$ exhibits the characteristics of a spiked Fisher matrix as described in [18]. Therefore, in the following section, we will employ the spectral theory of the spiked Fisher matrix to develop a fast method for estimating the capacity based on the formula (6).

III. FISHER-SPIKED ESTIMATION FOR DETERMINING THE CAPACITY

Assume that $K_m/J_m \rightarrow \beta_m$ as both J_m and K_m tend to infinity. This section proposes a Fisher-Spiked Estimation (FISE) algorithm to determine the average capacity per cluster in (6) when $\beta_m \leq 1$, leveraging the spectral theory of spiked Fisher matrices. The capacity computation is divided into two parts. One part is achieved by the fast estimation of top R spiked eigenvalues, while the other part is estimated by the limiting spectral distribution of the remaining non-spiked eigenvalues.

A. The approximate signal model

As shown in (4) and (6), the uplink signal model of the m -th cluster involves Hadamard product $\mathbf{L}_m \circ \mathbf{G}_m$. However, existing studies on the Hadamard product, as discussed in [19]–[22], often yield results that are implicit and cannot directly apply to practical scenarios. Therefore, based on Theorem 1 in [11], we consider approximating the signal model (4) without the diagonal assumption of $\mathbf{\Xi}_m$ but preserving its randomness. We replace the Hadamard product $\mathbf{L}_m \circ \mathbf{G}_m$ with the matrix product $\tilde{\mathbf{L}}_m \mathbf{G}_m$, where

$$\tilde{\mathbf{L}}_m = \text{diag}(l_{m1k}, \dots, l_{mJ_mk}), \quad (7)$$

and $l_{mjk} = 1/K_m \sum_{k=1}^{K_m} l_{mjk}$. This approximation forms the foundation of the design of the FISE algorithm, and its optimality can be proven in the following lemma. The proof is similar to that of Theorem 1 in [11], except for the target matrix \mathbf{L}_m instead of their $\mathbf{Q}_m = P^{1/2}\mathbf{\Xi}_m^{-1/2}\mathbf{L}_m$.

Lemma 1. For any matrix $\check{\mathbf{L}}_m$, define

$$\mathbf{\Delta}_m = \mathbf{L}_m \circ \mathbf{G}_m - \check{\mathbf{L}}_m \mathbf{G}_m.$$

$\mathbb{E} (\|\mathbf{\Delta}_m\|_F^2)$ reaches the minimum value if and only if $\check{\mathbf{L}}_m$ takes the value of (7), and the minimum is

$$\mathbb{E} (\|\mathbf{\Delta}_m\|_F^2) |_{\min} = \sum_{j=1}^{J_m} \left[\sum_{k=1}^{K_m} l_{mjk}^2 - \frac{1}{K_m} \left(\sum_{k=1}^{K_m} l_{mjk} \right)^2 \right].$$

Lemma 1 demonstrates that the error between matrices $\mathbf{L}_m \circ \mathbf{G}_m$ and $\check{\mathbf{L}}_m \mathbf{G}_m$ is minimized when $\check{\mathbf{L}}_m$ takes the value specified in (7). By substituting $\mathbf{L}_m \circ \mathbf{G}_m$ with the matrix product $\check{\mathbf{L}}_m \mathbf{G}_m$, we shift our focus to calculating the following capacity approximation

$$\hat{C}_m = \mathbb{E} \left\{ \frac{1}{J_m} \log \det \left(\mathbf{I} + P \mathbf{\Xi}_m^{-1/2} \check{\mathbf{L}}_m \mathbf{G}_m \mathbf{G}_m^* \check{\mathbf{L}}_m^* \mathbf{\Xi}_m^{-1/2} \right) \right\}. \quad (8)$$

B. FISE algorithm for $\beta_m \leq 1$

For the approximate capacity given in (8), we first concentrate on the scenario where $\beta_m \leq 1$, i.e., $K_m \leq J_m$. Define $\mathbf{P}_m = P \mathbf{\Xi}_m^{-1/2} \check{\mathbf{L}}_m \mathbf{G}_m \mathbf{G}_m^* \check{\mathbf{L}}_m^* \mathbf{\Xi}_m^{-1/2}$, and we can obtain the spectral decomposition of the matrix $\mathbf{I} + \mathbf{P}_m$ as

$$\mathbf{I} + \mathbf{P}_m = \mathbf{U} \mathbf{\Lambda} \mathbf{U}^*,$$

where $\mathbf{\Lambda} = \text{diag}(\lambda_1, \dots, \lambda_{J_m})$ is a diagonal matrix with the descending eigenvalues of $\mathbf{I} + \mathbf{P}_m$, and \mathbf{U} is a $J_m \times J_m$ unitary matrix consisting of the corresponding eigenvectors. Then, the capacity \hat{C}_m in (8) can be determined by summing the logarithms of eigenvalues:

$$\hat{C}_m = \frac{1}{J_m} \mathbb{E} \{ \log \det (\mathbf{I} + \mathbf{P}_m) \} = \frac{1}{J_m} \sum_{j=1}^{J_m} \mathbb{E} \{ \log (\lambda_j) \}. \quad (9)$$

As mentioned in Section II, the matrix $\mathbf{I} + \mathbf{P}_m$ can also be rewritten as $\mathbf{\Sigma}_1 \mathbf{\Sigma}_2^{-1}$, where $\mathbf{\Sigma}_1 = \mathbf{\Sigma}_2 + \mathbf{\Delta}$ and $\mathbf{\Delta} = \mathbf{P}_m \mathbf{\Sigma}_2$. Therefore, the matrix $\mathbf{I} + \mathbf{P}_m$ is also of the spiked Fisher matrix type, when \mathbf{P}_m is a low rank matrix. We denote the rank of the matrix \mathbf{P}_m as R , then $R \leq \min(J_m, K_m)$. Further, $\text{rank}(\mathbf{\Delta}) = \text{rank}(\mathbf{P}_m) = R$. If R is small compared to J_m , $\mathbf{\Sigma}_1 \mathbf{\Sigma}_2^{-1}$ is a standard spiked Fisher matrix that has been extensively studied in the literature, such as [23], [24]. If R diverges as J_m approaches infinity but still exhibits a few dominant eigenvalues, $\mathbf{\Sigma}_1 \mathbf{\Sigma}_2^{-1}$ remains a spiked Fisher matrix with a diverging number of spikes, as discussed in [25] and [26].

For each observation of $\mathbf{I} + \mathbf{P}_m$ in practical scenarios, we can similarly rewrite it in the form of $\mathbf{S}_1\mathbf{S}_2^{-1}$, where \mathbf{S}_1 and \mathbf{S}_2 are regarded as the corresponding sample covariance matrices of Σ_1 and Σ_2 , respectively. Thus, we study the sample limiting properties of $\mathbf{S}_1\mathbf{S}_2^{-1}$ to capture the underlying population information. Denote the descending eigenvalues of $\mathbf{S}_1\mathbf{S}_2^{-1}$ by $\rho_1 \geq \rho_2 \geq \dots \geq \rho_{J_m}$, then the capacity in (9) can be further approximated as

$$\widehat{C}_m \approx \frac{1}{J_m} \sum_{j=1}^{J_m} \mathbb{E} \{ \log \rho_j \}. \quad (10)$$

Distinguishing from [11], which requires selecting the number of spiked eigenvalues by adjusting parameters in advance, this study is free of tuning parameters. We just assume that the number of spikes in $\mathbf{S}_1\mathbf{S}_2^{-1}$ is exactly R , the rank of the matrix \mathbf{P}_m . According to [18], as $J_m, K_m \rightarrow \infty$, $K_m/J_m \rightarrow \beta_m \in (0, 1)$, and $J_m/(K - K_m) \rightarrow y_m \in (0, 1)$, the limiting spectral distribution (LSD) generated from the $J_m - R$ non-spiked eigenvalues of $\mathbf{S}_1\mathbf{S}_2^{-1}$ has the following density function

$$p_{\beta_m, y_m}(x) = \begin{cases} \frac{\beta_m(1-y_m)}{2\pi x(1+\beta_my_mx)} \sqrt{(b_m-x)(x-a_m)}, & a_m \leq x \leq b_m, \\ 0, & \text{else,} \end{cases} \quad (11)$$

and has a point mass $1 - \beta_m$ at the origin, where $a_m, b_m = (1 \mp \mu)^2 / (1 - y_m)^2$ with $\mu = \sqrt{(1 + \beta_my_m - y_m)/\beta_m}$. As discussed in [18], the top R spiked eigenvalues are located outside the support set $[a_m, b_m]$, while the rest $J_m - R$ non-spiked eigenvalues lie within the interval $[a_m, b_m]$. Therefore, the capacity expression in (10) can be further split into two terms as

$$\widehat{C}_m \approx \frac{1}{J_m} \mathbb{E} \left\{ \sum_{j=1}^R \log \rho_j \right\} + \frac{1}{J_m} \mathbb{E} \left\{ \sum_{k=R+1}^{J_m} \log \rho_k \right\} \triangleq C_{m1} + C_{m2}. \quad (12)$$

Then, we will provide the estimates for C_{m1} and C_{m2} separately.

We first concentrate on estimating C_{m1} . As aforementioned, the spiked eigenvalues $\rho_1 \geq \rho_2 \geq \dots \geq \rho_R$ are outside of the support set $[a_m, b_m]$ as $J_m, K_m \rightarrow \infty$ and $K_m/J_m \rightarrow \beta_m$. These eigenvalues are expected to be greater than b_m , thus b_m can be regarded as their lower bound, that is, $\rho_1 \geq \rho_2 \geq \dots \geq \rho_R > b_m$. For simple calculation, we suppose that $\rho_1, \rho_2, \dots, \rho_R$ are evenly spaced outside the support set with an equal step of $\Delta\rho$, then we can obtain their estimates as

$$\hat{\rho}_j = b_m + (R + 1 - j)\Delta\rho, j = 1, 2, \dots, R. \quad (13)$$

These eigenvalues should satisfy

$$\sum_{j=1}^R \hat{\rho}_j \approx R + \text{tr}(\mathbf{P}_m). \quad (14)$$

Combining the formulas (13) and (14), we can obtain the value of the step $\Delta\rho$ as

$$\Delta\rho = \frac{2(\text{tr}(\mathbf{P}_m) + R - Rb_m)}{R(R+1)}. \quad (15)$$

By substituting (15) into (13), the values of all approximate spiked eigenvalues $\hat{\rho}_j, j = 1, \dots, R$ can be obtained. Consequently, C_{m1} in (12) can be estimated by

$$\hat{C}_{m1} = \frac{1}{J_m} \sum_{j=1}^R \log \hat{\rho}_j. \quad (16)$$

Next, to estimate C_{m2} , we utilize the LSD of the Fisher matrix as defined in (11). The term C_{m2} is calculated by the $J_m - R$ non-spiked eigenvalues $\rho_{R+1}, \dots, \rho_{J_m}$, which are located within the support set of the LSD. Furthermore, since \mathbf{P}_m is a non-negative definite matrix, the eigenvalues of $\mathbf{I} + \mathbf{P}_m$ should be greater than 1. Then, by the spectra convergence in the Fisher matrix, C_{m2} can be approximated by the following integral

$$\hat{C}_{m2} = \int_{\max(1, a_m)}^{b_m} \log(x) p_{\beta_m, y_m}(x) dx. \quad (17)$$

Finally, an estimation of the capacity in (10) is obtained by combining the results from (16) and (17).

The algorithm for determine C_m for $\beta_m \leq 1$ is summarized as below.

Algorithm 1 Fisher-Spiked Estimation (FISE)

Input: $\mathbf{P}_m, K, J_m, K_m, R$.

Output: Estimation of C_m .

- 1: Calculate $\text{tr}(\mathbf{P}_m)$.
 - 2: Calculate $\Delta\rho = 2[\text{tr}(\mathbf{P}_m) + R - Rb_m]/[R(R+1)]$, where R is the rank of \mathbf{P}_m and b_m is the right endpoint of the support set in the density function in (11).
 - 3: Compute $\hat{\rho}_j = b_m + (R+1-j)\Delta\rho, j = 1, \dots, R$.
 - 4: Compute \hat{C}_{m1} according to (16).
 - 5: Compute \hat{C}_{m2} according to (17).
 - 6: Add \hat{C}_{m2} to \hat{C}_{m1} , and the sum is used as the estimation of C_m .
-

It is worth mentioning that, according to the algorithm procedure, the time complexity of the FISE algorithm amounts to $O(J_m)$, which is equivalent to the complexity of TOSE, lower than the complexity of the MPM algorithm $O(J_m^2)$, and much lower than that of determinant-calculation-based methods $O(J_m^3)$.

IV. CAPACITY STABILITY FOR $\beta_m > 1$

This section introduces a simplified capacity estimate that requires only basic computations when $\beta_m > 1$. We then theoretically prove that this estimation is a constant value, which is free of the parameter β_m .

The Lemma 1 in [4] states that the matrix $\Xi_m^{-1/2} \mathbf{H}_m \mathbf{H}_m^* \Xi_m^{-1/2}$ converges to a positive definite diagonal matrix \mathbf{R}_m as K_m approach infinity, where

$$\mathbf{R}_m = \text{diag}(r_{11}, \dots, r_{jj}, \dots, r_{J_m J_m})$$

with

$$r_{jj}^m = \frac{\sum_{u_k \in \mathcal{C}_m} l_{mjk}^2}{N_0 + P \sum_{u_k \notin \mathcal{C}_m} l_{mjk}^2}.$$

However, as mentioned in the Introduction, for small values of $\beta_m < 1$, even if a large-dimensional matrix converges to a limiting matrix, its corresponding spectrum does not converge to that of the limiting matrix. Thus, the diagonal limiting assumption for the matrix $\Xi_m^{-1/2} \mathbf{H}_m \mathbf{H}_m^* \Xi_m^{-1/2}$ results in significant errors in capacity estimation. But when $\beta_m > 1$, the error between the two spectra decreases as β_m increases. Therefore, the following expression can be regarded as a reasonable estimate of C_m for large $\beta_m > 1$.

$$\begin{aligned} \tilde{C}_m &= \lim_{K_m \rightarrow \infty} \mathbb{E} \left\{ \frac{1}{J_m} \log_2 \det(\mathbf{I} + P \mathbf{R}_m) \right\} \\ &= \lim_{K_m \rightarrow \infty} \frac{1}{J_m} \sum_{j=1}^{J_m} \log_2 \left(1 + \frac{P \sum_{u_k \in \mathcal{C}_m} l_{mjk}^2}{N_0 + P \sum_{u_k \notin \mathcal{C}_m} l_{mjk}^2} \right). \end{aligned} \quad (18)$$

Hence, the expression (18) provides a straightforward approach to computing the capacity, reducing the complexity from high-dimensional matrix operations to simple numerical calculations.

When calculating capacity for the different values of β_m , the method given in [4] involves performing a repeated calculation for each β_m according to formula (18). However, we find that the capacity estimate (18) is actually a stable value, and we can utilize the property thereby avoiding repeated calculations. To prove this in detail, we introduce the following transformation.

Under the assumption of $K_m \rightarrow \infty$, the expression of r_{jj}^m can be transformed by replacing the discrete distributions of the network nodes with continuous density as follows.

$$\lim_{K_m \rightarrow \infty} \frac{\sum_{u_k \in \mathcal{C}_m} l_{mjk}^2}{N_0 + P \sum_{u_k \notin \mathcal{C}_m} l_{mjk}^2} = \frac{\int_{\mathbf{y} \in \mathcal{D}_m} f(\mathbf{x} - \mathbf{y}) \rho_u(\mathbf{y}) d\mathbf{y}}{N_0 + P \int_{\mathbf{y} \in \mathcal{D}_0 \setminus \mathcal{D}_m} f(\mathbf{x} - \mathbf{y}) \rho_u(\mathbf{y}) d\mathbf{y}}, \quad (m = 1, 2, \dots, J_m),$$

where \mathcal{D}_0 denotes the two-dimensional region spanning the entire network, and $\mathcal{D}_m \subseteq \mathcal{D}_0$ denotes the region spanned by the m -th cluster. Additionally, \mathbf{x} and \mathbf{y} represent the location coordinates of the BSs and users, respectively, $\rho_u(\mathbf{y})$ is the density function of users distributed over \mathcal{D}_0 , and $f(\mathbf{x} - \mathbf{y}) = \gamma d_{\mathbf{x}\mathbf{y}}^{-\epsilon}$, where

$$\gamma = \begin{cases} 1, & d_{\mathbf{x}\mathbf{y}} > d_1, \\ d_1^{-1.5}, & d_0 < d_{\mathbf{x}\mathbf{y}} \leq d_1, \\ d_1^{-1.5} d_0^{-2}, & 0 < d_{\mathbf{x}\mathbf{y}} \leq d_0, \end{cases} \quad \epsilon = \begin{cases} 3.5, & d_{\mathbf{x}\mathbf{y}} > d_1, \\ 2, & d_0 < d_{\mathbf{x}\mathbf{y}} \leq d_1, \\ 0, & 0 < d_{\mathbf{x}\mathbf{y}} \leq d_0. \end{cases}$$

Thus, the average cluster capacity estimation per BS is given by [4]

$$\tilde{C}_m = \log \frac{\frac{N_0}{P} + \int_{\mathbf{y} \in \mathcal{D}_0} f(\mathbf{x}_{mj} - \mathbf{y}) \rho_u(\mathbf{y}) d\mathbf{y}}{\frac{N_0}{P} + \int_{\mathbf{y} \in \mathcal{D}_0 \setminus \mathcal{D}_m} f(\mathbf{x}_{mj} - \mathbf{y}) \rho_u(\mathbf{y}) d\mathbf{y}}, \quad (19)$$

for some BS b_j in the m -th cluster with coordinate denoted by \mathbf{x}_{mj} .

By replacing the discrete distributions of the network nodes with continuous density and focusing on the interference-limited regime, where the background noise is negligible, we can prove that the average cluster capacity estimation in (18) is a stable value that remains invariant with respect to β_m , as described in the following theorem.

Theorem 1. *For ultra-dense wireless networks, the average cluster capacity estimate per BS $\tilde{C}_m(\beta_m)$ is a constant value that is independent of $\beta_m (> 1)$, where $\tilde{C}_m(\beta_m)$ is calculated using formula (18) corresponding to the ratio β_m . Specifically, for any two values $\beta_{m1} \neq \beta_{m2}$ and $\beta_{m1}, \beta_{m2} > 1$, the conclusion that $\tilde{C}_m(\beta_{m1}) = \tilde{C}_m(\beta_{m2})$ holds.*

Proof. If no confusion, represent $\rho_{\beta_m}(\mathbf{y})$ as the value of $\rho_u(\mathbf{y})$ at β_m . Then the average cluster capacity estimate at $\beta_{m1} > 1$ can be obtained as

$$\tilde{C}_m(\beta_{m1}) = \log \frac{\frac{N_0}{P} + \int_{\mathbf{y} \in \mathcal{D}_0} f(\mathbf{x}_{mj} - \mathbf{y}) \rho_{\beta_{m1}}(\mathbf{y}) d\mathbf{y}}{\frac{N_0}{P} + \int_{\mathbf{y} \in \mathcal{D}_0 \setminus \mathcal{D}_m} f(\mathbf{x}_{mj} - \mathbf{y}) \rho_{\beta_{m1}}(\mathbf{y}) d\mathbf{y}}. \quad (20)$$

Since

$$\int_{\mathbf{y} \in \mathcal{D}_m} \rho_{\beta_m}(\mathbf{y}) d\mathbf{y} = K_m = \beta_m J_m, \quad (21)$$

thus $\int_{\mathbf{y} \in \mathcal{D}_m} \rho_{\beta_m}(\mathbf{y}) / \beta_m d\mathbf{y} = J_m$. By setting J_m to a large and fixed value, we isolate the quantity β_m to study its impact on network capacity $\tilde{C}_m(\beta_m)$. Therefore, when the distribution of user nodes remains unchanged, an increase in β_m will lead to a proportional increase in density $\rho_{\beta_m}(\mathbf{y})$, i.e.

$$\frac{\rho_{\beta_{m2}}(\mathbf{y})}{\rho_{\beta_{m1}}(\mathbf{y})} = \frac{\beta_{m2}}{\beta_{m1}},$$

where $\beta_{m2} \neq \beta_{m1}$ and $\beta_{m1}, \beta_{m2} > 1$. Therefore, $\tilde{C}_m(\beta_{m2})$ can be calculated as

$$\begin{aligned} \tilde{C}_m(\beta_{m2}) &= \log \frac{\frac{N_0}{P} + \int_{\mathbf{y} \in \mathcal{D}_0} f(\mathbf{x}_{mj} - \mathbf{y}) \rho_{\beta_{m2}}(\mathbf{y}) d\mathbf{y}}{\frac{N_0}{P} + \int_{\mathbf{y} \in \mathcal{D}_0 \setminus \mathcal{D}_m} f(\mathbf{x}_{mj} - \mathbf{y}) \rho_{\beta_{m2}}(\mathbf{y}) d\mathbf{y}} \\ &= \log \frac{\frac{N_0}{P} + \frac{\beta_{m2}}{\beta_{m1}} \int_{\mathbf{y} \in \mathcal{D}_0} f(\mathbf{x}_{mj} - \mathbf{y}) \rho_{\beta_{m1}}(\mathbf{y}) d\mathbf{y}}{\frac{N_0}{P} + \frac{\beta_{m2}}{\beta_{m1}} \int_{\mathbf{y} \in \mathcal{D}_0 \setminus \mathcal{D}_m} f(\mathbf{x}_{mj} - \mathbf{y}) \rho_{\beta_{m1}}(\mathbf{y}) d\mathbf{y}} \\ &= \log \frac{\frac{N_0}{P} \frac{\beta_{m1}}{\beta_{m2}} + \int_{\mathbf{y} \in \mathcal{D}_0} f(\mathbf{x}_{mj} - \mathbf{y}) \rho_{\beta_{m1}}(\mathbf{y}) d\mathbf{y}}{\frac{N_0}{P} \frac{\beta_{m1}}{\beta_{m2}} + \int_{\mathbf{y} \in \mathcal{D}_0 \setminus \mathcal{D}_m} f(\mathbf{x}_{mj} - \mathbf{y}) \rho_{\beta_{m1}}(\mathbf{y}) d\mathbf{y}} \end{aligned} \quad (22)$$

When the background noise is ignored, the expressions (20) and (22) are equivalent, i.e.

$$\tilde{C}_m(\beta_{m2}) = \tilde{C}_m(\beta_{m1}).$$

The proof is completed. \square

Theorem 1 implies that the estimated capacity \tilde{C}_m stabilizes and does not vary with further increases in β_m . Therefore, for $\beta_m > 1$, the estimation of the capacity \tilde{C}_m can be calculated only once using the simplified formula in (18), avoiding the repeated calculations for each β_m . Then, this estimation will approach the real value of the capacity C_m with increasing β_m , as illustrated by the experimental study detailed in Section IV. This is significant for simplifying the analysis and optimization of ultra-dense networks where β_m can vary widely.

According to (21), the explicit relationship between $\rho_{\beta_m}(\mathbf{y})$ and β_m is difficult to obtain. Consequently, deriving an explicit expression for \tilde{C}_m in (19) is formidable. However, when the user nodes are uniformly distributed, a specific limit expression of \tilde{C}_m can be determined by the following corollary under the more general condition than in Theorem 1, i.e., without ignoring background noise.

Corollary 1. *Assuming that the user density is a constant and the numbers of BSs and users approach infinity, the average cluster capacity per BS is estimated by*

$$\tilde{C}_m = \log \frac{\int_{\mathbf{y} \in \mathcal{D}_0} f(\mathbf{x}_{mj} - \mathbf{y}) d\mathbf{y}}{\int_{\mathbf{y} \in \mathcal{D}_0 \setminus \mathcal{D}_m} f(\mathbf{x}_{mj} - \mathbf{y}) d\mathbf{y}}. \quad (23)$$

Proof. When the user density is a constant, we simplify $\rho_u(\mathbf{y})$ as ρ_u , which can be directly calculated as

$$\rho_u = \frac{K_m}{|\mathcal{D}_m|}.$$

Here, $|\mathcal{D}_m|$ denotes the area of \mathcal{D}_m with a slight abuse of notation. Then, the average cluster capacity per BS is estimated by

$$\begin{aligned} \tilde{C}_m &= \log \frac{\frac{N_0}{P} + \int_{\mathbf{y} \in \mathcal{D}_0} f(\mathbf{x}_{mj} - \mathbf{y}) \rho_u(\mathbf{y}) d\mathbf{y}}{\frac{N_0}{P} + \int_{\mathbf{y} \in \mathcal{D}_0 \setminus \mathcal{D}_m} f(\mathbf{x}_{mj} - \mathbf{y}) \rho_u(\mathbf{y}) d\mathbf{y}} \\ &= \log \frac{\frac{N_0}{P} + \frac{K_m}{|\mathcal{D}_m|} \int_{\mathbf{y} \in \mathcal{D}_0} f(\mathbf{x}_{mj} - \mathbf{y}) d\mathbf{y}}{\frac{N_0}{P} + \frac{K_m}{|\mathcal{D}_m|} \int_{\mathbf{y} \in \mathcal{D}_0 \setminus \mathcal{D}_m} f(\mathbf{x}_{mj} - \mathbf{y}) d\mathbf{y}} \\ &= \log \frac{\frac{N_0 |\mathcal{D}_m|}{P K_m} + \int_{\mathbf{y} \in \mathcal{D}_0} f(\mathbf{x}_{mj} - \mathbf{y}) d\mathbf{y}}{\frac{N_0 |\mathcal{D}_m|}{P K_m} + \int_{\mathbf{y} \in \mathcal{D}_0 \setminus \mathcal{D}_m} f(\mathbf{x}_{mj} - \mathbf{y}) d\mathbf{y}}. \end{aligned} \quad (24)$$

Even if the background noise N_0 is not negligible, the term $N_0|\mathcal{D}_m|/(PK_m)$ still tends to 0 due to the asymptotic assumption of $K_m \rightarrow \infty$. The expression (24) can thus be written as

$$\tilde{C}_m = \log \frac{\int_{\mathbf{y} \in \mathcal{D}_0} f(\mathbf{x}_{mj} - \mathbf{y}) d\mathbf{y}}{\int_{\mathbf{y} \in \mathcal{D}_0 \setminus \mathcal{D}_m} f(\mathbf{x}_{mj} - \mathbf{y}) d\mathbf{y}}. \quad (25)$$

The proof is completed. \square

We note that in [4], the same result as (23) was derived under the assumption of negligible background noise. Conversely, our work establishes that the conclusion of Corollary 1 holds even under the more general condition where background noise is considered.

V. PERFORMANCE EVALUATION

In this section, numerical simulations are conducted to assess the high efficiency and exceptional generality of our proposed methods for capacity determination.

A. Network settings

In our simulations, we explore two kinds of ultra-dense wireless network scenarios. The detailed designs of these scenarios are as follows, with visualizations provided in Fig. 2.

- S1. The network is circular with a diameter of $2D$. The locations of BSs and users obey a homogeneous Poisson point process (PPP) with intensity Λ_b and Λ_u [27]. Therefore, J and K follow Poisson distributions:

$$\text{P}(J \text{ BSs in region } \mathcal{D}_0) = \frac{(\Lambda_b \alpha)^J e^{-\Lambda_b \alpha}}{\Gamma(J+1)} \text{ and } \text{P}(K \text{ users in region } \mathcal{D}_0) = \frac{(\Lambda_u \alpha)^K e^{-\Lambda_u \alpha}}{\Gamma(K+1)},$$

where $\alpha = \pi D^2$. Moreover, the distance of the j -th node from the center is a random variable (RV) with the probability distribution function (PDF)

$$f_1(D; t) = \frac{2t}{D^2}, 0 \leq t \leq D.$$

S2. The network is square with a side length of $2D$, and both components of the j -th node's location, (x_j, y_j) , are RVs with the truncated normal distribution function

$$f_2(\mu, \sigma, -D, D; t) = \begin{cases} \frac{\phi(\mu, \sigma^2; t)}{\Phi(\mu, \sigma^2; D) - \Phi(\mu, \sigma^2; -D)}, & -D \leq t \leq D; \\ 0, & \text{other,} \end{cases}$$

where $\phi(\cdot)$ and $\Phi(\cdot)$ represent the PDF and cumulative distribution function (CDF) of the normal distribution, respectively. The parameters μ and σ are the mean and variance of the normal distribution.

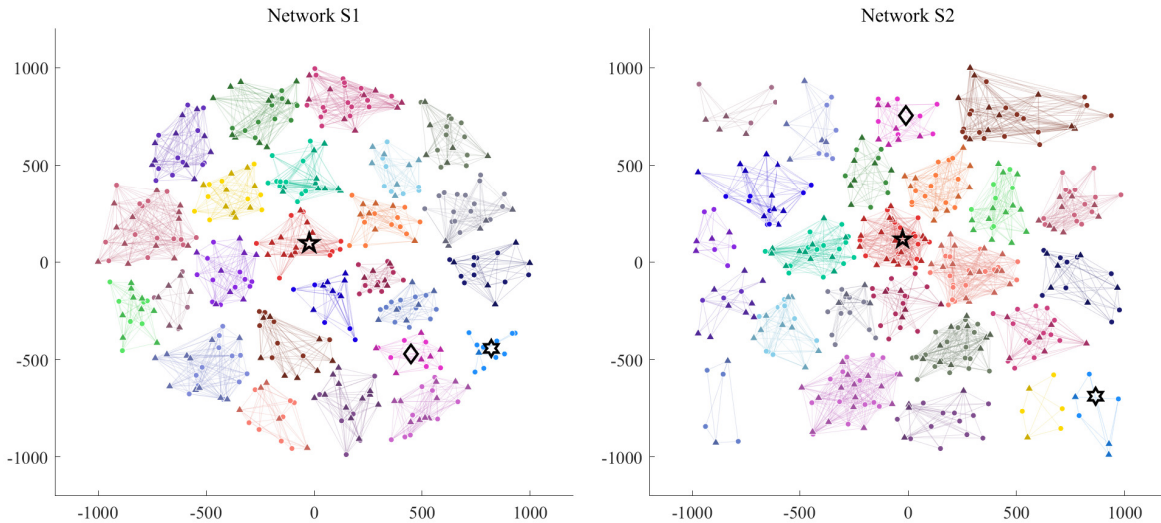


Fig. 2. Visualization of C^2 architectures under different network settings. Triangles are users, and circles are BSs. Each color represents a cluster. The clusters marked by the black pentagon, the black diamond, and the black hexagon correspond to the cluster closest to the network center, the cluster at the median position³, and the cluster furthest from the network center, respectively.

In network S1, the intensity of BSs is given by $\Lambda_b = \Omega/(\pi D^2)$, where Ω is a positive integer, representing the average number of BSs in the region of πD^2 . With a given Λ_b , the intensity of

³Calculate the distances of all clusters to the network center and sort them in descending order, the cluster corresponding to the median is the one we consider.

users can be calculated according to $\Lambda_u = \Lambda_b \beta$ [4], where β represents the ratio of the number of users to the number of BSs in the entire network. In our two network scenarios, the distribution of users and BSs is exactly the same, so the β_m value in the m -th cluster is theoretically equal to the β value in the entire network. Due to the randomness of simulations, β_m is around and approximately equal to β . In the following experimental analysis, for convenience, we record it as $\beta_m = \beta$.

In network S1, nodes are uniformly distributed, meaning the density of nodes remains constant regardless of the distance from the network center. This is a classical distribution in wireless networks. Conversely, in network S2, nodes follow a truncated normal distribution, which implies that the density of nodes decreases as the distance from the network center increases. This setup mimics real-world scenarios, with a higher concentration of nodes in the central urban area and fewer nodes in the surrounding rural area.

As shown in Fig. 2, the entire network is partitioned into M non-overlapping clusters using the K-means algorithm [28]. To further validate the generality of our methods, we select three clusters based on their proximity to the network center: the cluster closest to the network center, the cluster at the median position, and the cluster furthest from the network center. The average capacity is then estimated by averaging over 200 replications for each network scenario. The setting of basic network parameters is shown in Table I below.

TABLE I
THE NETWORK SETTING

Definition and Symbol	Value
Network scale (D)	1000 m
Near field threshold (d_0)	10 m
Far field threshold (d_1)	50 m
Transmit power (P)	1 W
Noise power (N_0)	1×10^{-12} W
Number of clusters (M)	25
Mean and variance in S2 (μ, σ^2)	(0, 600^2)

B. Performance evaluation of our methods

To evaluate the performance of our proposed methods, we compare the capacity obtained by our approach with those obtained by TOSE [11] and MPM [12], with Cholesky decomposition

as the baseline. According to [11], TOSE requires the selection of the ratio of spiked eigenvalues used in the algorithm, which recommends the ratio value set to 0.7. In addition, the MPM method in [12] approximates the channel capacity by an integral form, which requires the choice of the parameter η involved in the lower limit. They suggest that 4×10^{-3} is a relatively optimal choice for all cases. Compared to these two methods, our methods offer the advantage of not requiring any parameter tuning.

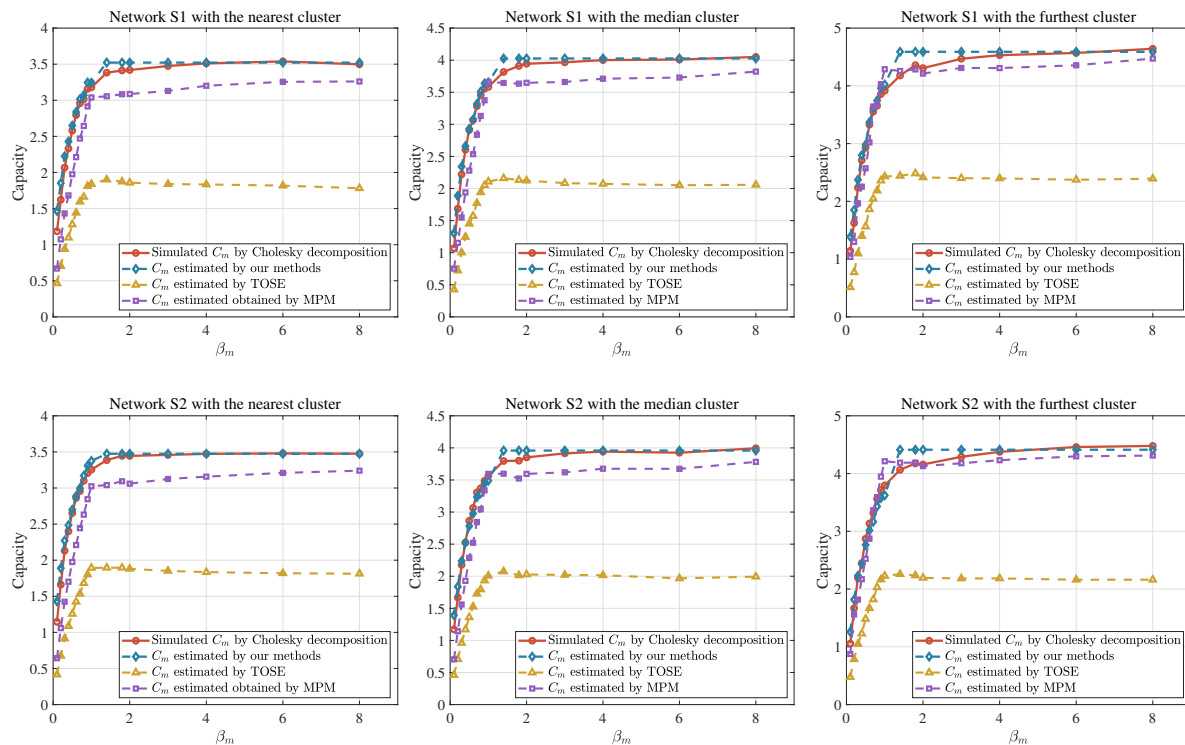


Fig. 3. The comparison of the capacity obtained by our methods (blue diamond), TOSE (yellow triangle), MPM (purple square), and Cholesky decomposition (red circle). The $\beta_m \leq 1$ part of the blue line is obtained by the FISE algorithm, and the $\beta_m > 1$ part is calculated by the formula (18). The first and second rows correspond to the networks S1 and S2. The left, middle, and right columns correspond to the location of clusters closest to the network center, at the median position, and furthest from the network center, respectively.

Fig. 3 illustrates the capacity comparisons obtained by different methods as β_m increases, using Cholesky decomposition as the baseline for simulating the precise values of C_m according to equation (6). In network S1, the intensity of BSs is fixed at $\Lambda_b = 10^{-3}$. In network S2, the total number of BSs J across the entire network is set to 5000. The line with blue diamonds in the figure represents the capacity estimate obtained by our methods. Specifically, the capacity

for $\beta_m \leq 1$ is obtained using the FISE algorithm. For $\beta_m > 1$, we select the capacity estimate \tilde{C}_m when $\beta_m = 3$, $\tilde{C}_m(3)$, to replace the capacity estimates under all the values of $\beta_m > 1$.

As depicted in the Fig. 3, our proposed methods exhibit superior performance relative to all other methods assessed. On the one hand, it is observed that the FISE method has high accuracy when $\beta_m \leq 1$, with a relative error in capacity from the baseline results (represented by red circles) of less than 2%. Conversely, the TOSE method (represented by yellow triangles) shows significantly poorer performance. Although the capacity estimation obtained by MPM (represented by purple squares) outperforms TOSE, it still exhibits greater errors compared to our methods. The errors in MPM stem from the assumption of diagonal noise-plus-interference matrix in the limiting regime, which might not hold accurately for small β_m , as discussed in the Introduction. On the other hand, using the capacity estimates $\tilde{C}_m(3)$ to replace capacity estimates for all $\beta_m > 1$ results in remarkable accuracy across various network settings. As β_m increases, the estimation becomes increasingly accurate and is almost the same as the baseline result, which verifies the validity of Theorem 1.

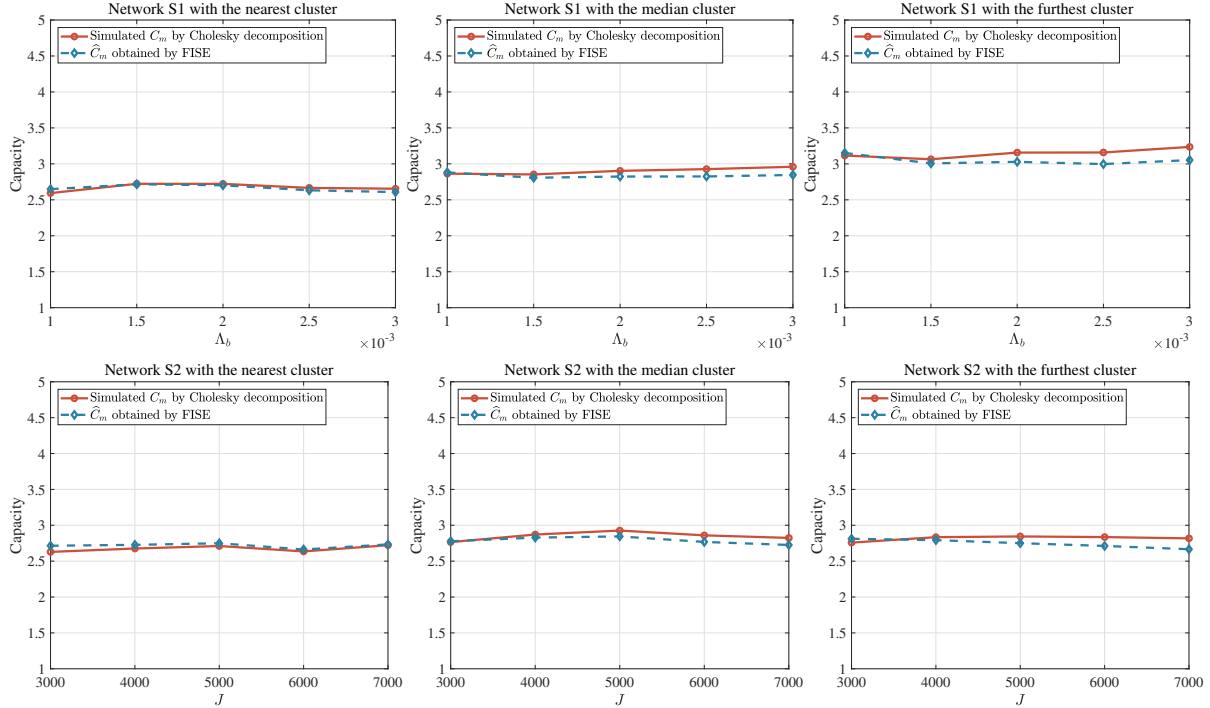


Fig. 4. The comparison of the capacity calculated by Cholesky decomposition (Solid line) and FISE (dashed line) when $\beta_m = 0.5$. The first and second rows correspond to the networks S1 and S2. The left, middle, and right columns correspond to the location of clusters closest to the network center, at the median position, and furthest from the network center, respectively.

In Fig. 4–5, we plot to compare the capacity achieved using our proposed methods versus the Cholesky decomposition method by increasing the density of nodes while maintaining a fixed value of β_m , equivalently fixed β . Specifically, in network S1, we augment the node density by varying the intensity of BSs, Λ_b . Simultaneously, we increase the intensity of users according to $\Lambda_u = \Lambda_b\beta$. For network S2, the density of nodes is escalated by increasing the number of BSs, J , while proportionally increasing the number of users to $K = J\beta$. Fig. 4 shows the capacity comparison in different scenarios for $\beta_m = 0.5$, and Fig. 5 depict similar results for $\beta_m = 4$. It can be observed that the capacity estimation remains nearly constant with a fixed β_m . Our proposed estimates closely align with baseline results across all scenarios, demonstrating high accuracy and robustness suitable for real-world deployments.

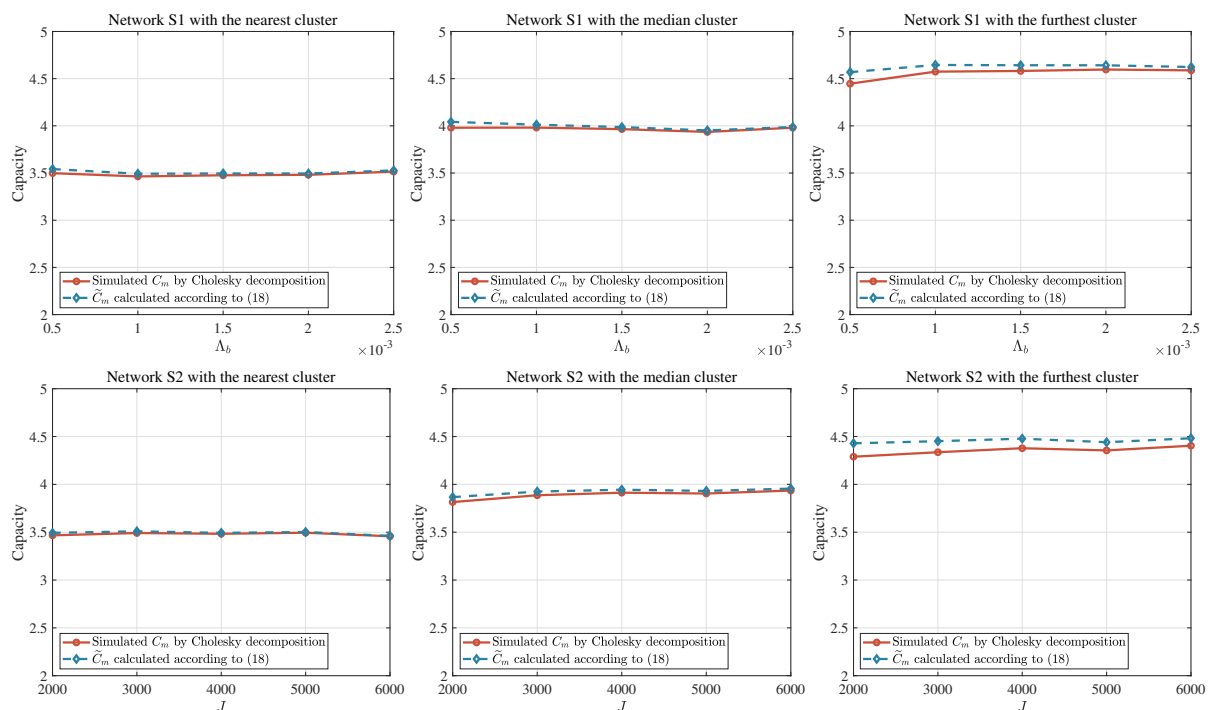


Fig. 5. The comparison of the capacity calculated by Cholesky decomposition (Solid line) and the formula (18) (dashed line) when $\beta_m = 4$. The first and second rows correspond to the networks S1 and S2. The left, middle, and right columns correspond to the location of clusters closest to the network center, at the median position, and furthest from the network center, respectively.

Furthermore, Fig. 3–5 also demonstrate the generality of our proposed methods. They exhibit high accuracy across different network node distributions, network area shapes, cluster locations, and different values of β_m .

VI. CONCLUSION

This paper develops efficient methods for estimating the channel capacity in future ultra-dense wireless networks with random interference, which are fast, accurate and general. For $\beta_m \leq 1$, the FISE algorithm is proposed to realize the fast estimation of eigenvalues by treating the interference as random. According to the analysis, the FISE algorithm has a linear time complexity, much lower than the polynomial time of most existing methods. For $\beta_m > 1$, we introduce a computationally simple expression for capacity estimation and prove that it is a stable value that is independent of β_m . The estimations are also almost the same as the baseline results but with reduced complexity. Numerical experiments demonstrate the high accuracy and superior generality of our proposed methods. Regardless of the network shape, node distribution, and cluster location, our methods provide nearly identical capacity estimations to the baseline method. In future work, we will study the limiting theory of the Hadamard product between large-dimensional matrices involved in the signal model (4), further achieve even more efficient capacity estimations.

REFERENCES

- [1] C. E. Shannon, "A mathematical theory of communication," *The Bell System Technical Journal*, vol. 27, pp. 623–656, 1948.
- [2] T. M. Cover and J. A. Thomas, *Elements of Information Theory*, 2nd ed. John Wiley & Sons, Ltd, 2006.
- [3] E. Telatar, "Capacity of multi-antenna gaussian channels," *European Transactions on Telecommunications*, vol. 10, no. 6, pp. 585–595, 1999.
- [4] L. Yang, P. Li, M. Dong, B. Bai, D. Zaporozhets, X. Chen, W. Han, and B. Li, "C2: A capacity-centric architecture toward future wireless networking," *IEEE Transactions on Wireless Communications*, vol. 21, no. 10, pp. 8134–8147, 2022.
- [5] J. Wang, L. Dai, L. Yang, and B. Bai, "Rate-constrained network decomposition for clustered cell-free networking," in *IEEE International Conference on Communications (ICC 2022)*, 2022, pp. 2549–2554.
- [6] C. Deng, L. Yang, H. Wu, D. Zaporozhets, M. Dong, and B. Bai, "CGN: A capacity-guaranteed network architecture for future ultra-dense wireless systems," in *IEEE International Conference on Communications (ICC 2022)*, 2022, pp. 1853–1858.
- [7] L. Dai and B. Bai, "Optimal decomposition for large-scale infrastructure-based wireless networks," *IEEE Transactions on Wireless Communications*, vol. 16, no. 8, pp. 4956–4969, 2017.
- [8] M. Matthaiou, O. Yurduseven, H. Q. Ngo, D. Morales-Jimenez, S. L. Cotton, and V. F. Fusco, "The road to 6g: Ten physical layer challenges for communications engineers," *IEEE Communications Magazine*, vol. 59, no. 1, pp. 64–69, 2021.
- [9] J. Wang, L. Dai, L. Yang, and B. Bai, "Clustered cell-free networking: A graph partitioning approach," *IEEE Transactions on Wireless Communications*, vol. 22, no. 8, pp. 5349–5364, 2023.
- [10] A. Tulino and S. Verdú, "Random matrix theory and wireless communications," *Foundations and Trends in Communications and Information Theorists*, vol. 1, no. 1, 2004.

- [11] D. Jiang, L. Yang, H. Hao, and R. Wang, "TOSE: A fast capacity estimation algorithm based on spike approximations," in *2022 IEEE 96th Vehicular Technology Conference (VTC 2022-Fall)*, 2022, pp. 1–6.
- [12] H. Hao, D. Jiang, L. Yang, H. Wu, and B. Bai, "The moment passing method for wireless channel capacity estimation," in *2022 IEEE Global Communications Conference (GLOBECOM 2022)*, 2022, pp. 3605–3610.
- [13] R. Couillet and Z. Liao, *Random Matrix Methods for Machine Learning*. Cambridge University Press, 2022.
- [14] G. Interdonato, H. Q. Ngo, E. G. Larsson, and P. Frenger, "How much do downlink pilots improve cell-free massive mimo?" in *2016 IEEE Global Communications Conference (GLOBECOM)*, 2016, pp. 1–7.
- [15] M. Bashar, K. Cumanan, A. G. Burr, M. Debbah, and H. Q. Ngo, "On the uplink max–min sinr of cell-free massive mimo systems," *IEEE Transactions on Wireless Communications*, vol. 18, no. 4, pp. 2021–2036, 2019.
- [16] S. Buzzi, C. D'Andrea, A. Zappone, and C. D'Elia, "User-centric 5g cellular networks: Resource allocation and comparison with the cell-free massive mimo approach," *IEEE Transactions on Wireless Communications*, vol. 19, no. 2, pp. 1250–1264, 2020.
- [17] D. Tse and P. Viswanath, *Fundamentals of Wireless Communication*. Cambridge University Press, 2005.
- [18] Z. Bai and J. W. Silverstein, *Spectral Analysis of Large Dimensional Random Matrices*. Springer, 2010.
- [19] V. L. Girko, *Theory of Stochastic Canonical Equations*. Springer Science & Business Media, 2001.
- [20] W. Hachem, P. Loubaton, and J. Najim, "Deterministic equivalents for certain functionals of large random matrices," *The Annals of Applied Probability*, vol. 17, no. 3, pp. 875 – 930, 2007.
- [21] —, "A CLT for information-theoretic statistics of Gram random matrices with a given variance profile," *The Annals of Applied Probability*, vol. 18, no. 6, pp. 2071 – 2130, 2008.
- [22] J. W. Silverstein, "Limiting eigenvalue behavior of a class of large dimensional random matrices formed from a hadamard product," *Random Matrices: Theory and Applications*, vol. 12, no. 01, p. 2250050, 2023.
- [23] Q. Wang and J. Yao, "Extreme eigenvalues of large-dimensional spiked Fisher matrices with application," *The Annals of Statistics*, vol. 45, no. 1, pp. 415 – 460, 2017.
- [24] D. Jiang, Z. Hou, and J. Hu, "The limits of the sample spiked eigenvalues for a high-dimensional generalized fisher matrix and its applications," *Journal of Statistical Planning and Inference*, vol. 215, pp. 208–217, 2021.
- [25] J. Xie, Y. Zeng, and L. Zhu, "Limiting laws for extreme eigenvalues of large-dimensional spiked fisher matrices with a divergent number of spikes," *J. Multivar. Anal.*, vol. 184, no. C, jul 2021.
- [26] Y. Zeng and L. Zhu, "Order determination for spiked-type models with a divergent number of spikes," *Computational Statistics & Data Analysis*, vol. 182, p. 107704, 2023.
- [27] F. A. Khan, H. He, J. Xue, and T. Ratnarajah, "Performance analysis of cloud radio access networks with distributed multiple antenna remote radio heads," *IEEE Transactions on Signal Processing*, vol. 63, no. 18, pp. 4784–4799, 2015.
- [28] S. Lloyd, "Least squares quantization in pcm," *IEEE Transactions on Information Theory*, vol. 28, no. 2, pp. 129–137, 1982.